Available online at www.sciencedirect.com

SCIENCE DIRECT®

Engineering Geology 77 (2005) 139–151

ENGINEERING GEOLOGY

www.elsevier.com/locate/enggeo

# A preliminary probabilistic seismic hazard assessment in terms of Arias intensity in southeastern Spain

José A. Peláez[a,*], José Delgado[b], Carlos López Casado[c]

[a]Departamento de Física, Escuela Politécnica Superior, Universidad de Jaén, C/ Virgen de la Cabeza, 2, 23071 Jaén, Spain
[b]Departamento de Ciencias de la Tierra y del Medio Ambiente, Facultad de Ciencias, Universidad de Alicante, P.O. Box 99, 03080 Alicante, Spain
[c]Departamento de Física Teórica y del Cosmos, Facultad de Ciencias, Universidad de Granada, Avda. Severo Ochoa, s/n, 18071 Granada, Spain

Received 3 November 2003; accepted 7 September 2004

## Abstract

A preliminary probabilistic seismic hazard assessment in terms of Arias intensity is presented for the first time in southeastern Spain. In the calculation, the spatially smoothed seismicity procedure has been used, considering four seismic models, and a seismic catalog updated up to 1999. One of the models that include the most significant seismicity, considers earthquakes above 5.5 $M_S$ in the last 700 years.

Maps for a return period of 475 years, that is, for a 10% probability of exceedance in 50 years, and for different soil conditions, have been computed. The uncertainty in the final result is shown by depicting maps for the mean and mean+$\sigma$ attenuation curves. Independently of the geological soil conditions, higher Arias intensity values have been obtained along the Betic Cordilleras. The most significant result is the value obtained in the Granada Basin, the most active and hazardous Spanish seismogenic area. It is of the order of 0.4 m/s for shallow soils, 0.3 m/s for deep soils, and 0.2 m/s for stiff rock conditions, for the return period quoted above. These are typical values for a moderate seismic hazard region.


*Keywords:* Seismic hazard; Arias intensity; Spatially smoothed seismicity; Southeastern Spain; Landslides

## 1. Introduction

In recent years, and using the spatially smoothed seismicity methodology (Frankel, 1995), we have been able to reevaluate seismic hazard in Spain (Peláez and López Casado, 2002). In addition, seismic hazard deaggregation studies have been carried out at several significant places (Peláez et al., 2002; Peláez

* Corresponding author. Fax: +34 953212343.
*E-mail addresses:* japelaez@ujaen.es (J.A. Peláez), Jose.Delgado@ua.es (J. Delgado), clcasado@ugr.es (C. López Casado).

0013-7952/$ - see front matter © 2004 Elsevier B.V. All rights reserved.
doi:10.1016/j.enggeo.2004.09.002

and López Casado, 2004). Through this work, the computation of seismic hazard in terms of Arias intensity, we intend to continue seismic hazard studies in the south and southeastern Spain, the most seismically active and hazardous Spanish regions. This is an area that could be considered as having moderate seismic hazard (Peláez and López Casado, 2002). The obtained results are a step forward in an on-going research aimed to complete a probabilistic seismic–landslide hazard assessment utilizing both geological and geomorphological inputs. Moreover, they represent the first stage in a process of landslide spatial prediction (Corominas, 1993; Faccioli, 1995) whose goal is to answer the following questions: 'where will they occur?', or to be absolutely precise, 'where are they most likely?'

Mean peak ground acceleration (PGA) values (Fig. 1) are not a reliable parameter for dynamic slope stability studies. In such cases, it is very common to use the rigid block displacement model developed by Newmark (1965). In this model, the minimum ground acceleration required to overcome the maximum resistance of the slope to sliding is called the critical-acceleration. Nevertheless, it represents the acceleration for which shear stress and shear strength are in equilibrium along the assumed slip surface (Del Gaudio et al., 2003). Therefore, it uniquely describes the dynamic stability of a slope, being a measure of intrinsic slope properties (soil properties, groundwater and slope geometry) independent of any ground-shaking scenario (Jibson et al., 2000). This is the reason for using Newmarks's critical-acceleration only for susceptibility studies.

The Arias intensity (Arias, 1970) is a measure of earthquake intensity based on instrumental records, attempting to decrease the limitations of the empirical earthquake intensity scales, affected by many subjective elements. This is not the only instrumental intensity existing but it is also the most used one in earthquake triggered landslide studies based on the procedure developed by Newmark (e.g., Wilson and Keefer, 1985; Jibson et al., 1998, 2000; Romeo, 2000; Del Gaudio et al., 2003). The Arias intensity is also strongly correlated with the level of damage and local intensity (Margottini et al., 1992; Cabañas et al., 1997), the occurrence of different landslide categories

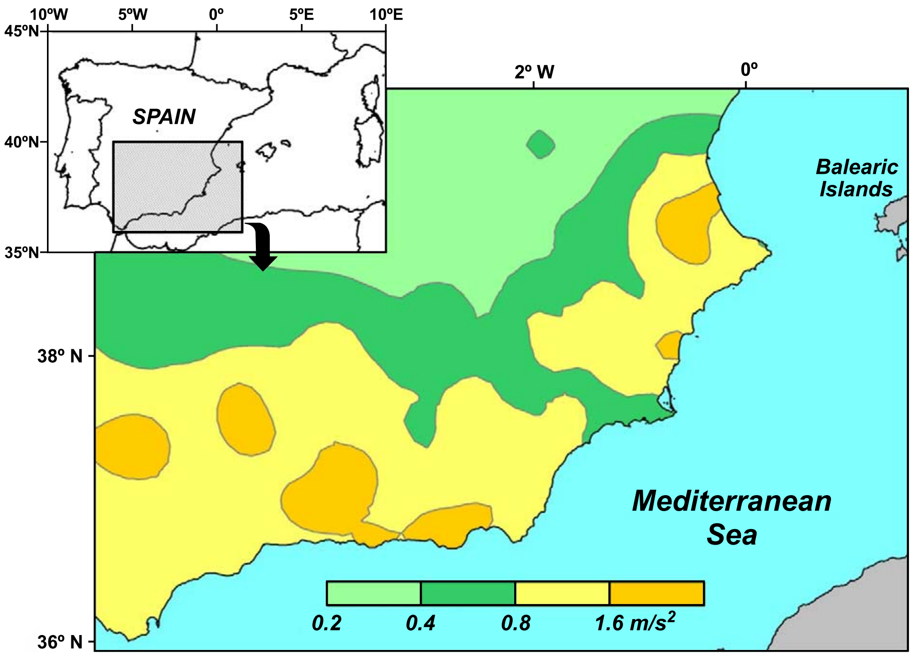


Fig. 1. Seismic hazard in terms of PGA in southeastern Spain: mean PGA for a return period of 475 years, i.e., with 10% probability of exceedance in 50 years (taken from Peláez and López Casado, 2002).

(Keefer and Wilson, 1989; Harp and Wilson, 1995), observed displacements (Carro et al., 2003), and liquefaction potential (Kayen and Mitchel, 1997a,b).

The Arias intensity was initially defined (Arias, 1970) as

$$\vartheta_I = \frac{\pi}{2g}\int_0^{t_0} a^2(t)\mathrm{d}t \tag{1}$$

and was called scalar intensity. It is directly quantifiable through the acceleration record $a(t)$, integrating it over the total duration of the earthquake. By definition, it is the trace of a second-order tensor. This is the reason why it is an invariant; therefore, it is not dependent on the accelerograph axis orientation. Unlike PGA, it considers the full range of frequencies recorded and included in the accelerogram and the duration of the ground motion. The Arias intensity is claimed to be a measure of the total seismic energy absorbed by the ground. Arias (1970) also defined the scalar intensity on the horizontal plane as

$$I_h = \frac{\pi}{2g}\int_0^{t_0} a_h^2(t)\mathrm{d}t \tag{2}$$

He pointed out the importance of this variable, because, among other reasons, man-made structures are more sensitive to horizontal ground motion than that vertical. Several landslide reports and field studies also use this last variable.

In this contribution, a case study, the method and results obtained in the assessment of probabilistic seismic hazard are presented in southeastern Spain, an area of active tectonics, in terms of Arias intensity. Specifically, we show the results for a return period of 475 years, that is, for a 10% probability of exceedance in 50 years, a return period usually considered in earthquake engineering studies. These results provide another assessment of regional probabilistic seismic hazard maps in terms of this variable such as those presented in recent years by Romeo (2000) and Abdrakhmatov et al. (2003). As stated above, the obtained results, a long-term seismic hazard assessment, are aimed at the identification or prediction of the limits affected by future earthquake-induced landsliding.

We think that these types of studies are very important in the south and southeast Spain. Although no significant earthquakes have been located in this region in recent decades, historic reports show clearly that this phenomenon occurred in the past, for instance as in the 1504 Carmona, the 1644 Muro de Alcoy, the 1680 NW Malaga, the 1829 Torrevieja, or in the 1884 Arenas del Rey earthquakes (Table 1). A detailed documentation and revision of these and other historic events in this region, including smaller uncertainties in the epicentral and maximum intensity determinations, will be a basis for understanding the hazard associated with earthquake triggered landslides (Keefer, 2002).

## 2. Tectonic setting

The area of study is found in the central and eastern sectors of the Betic Cordillera, which, together with the Rif Cordillera in north Africa, constitute the westernmost part of the Alpine Mediterranean chains. The Betic Cordillera can be divided into the Internal

Table 1
Earthquakes quoted in the text (taken from Martínez Solares and Mezcua, 2002)

| Date | Epicenter | Error (km) | Intensity | Location |
|---|---|---|---|---|
| 12/18/1396 | 00°03′W 39°05′N | 10–20 | VIII–IX | Tabernes de Valldigna (Valencia) |
| 04/24/1431 | 03°38′W 37°08′N | >50 | VIII–IX | Atarfe (Granada) |
| 04/05/1504 | 05°28′W 37°23′N | 20–50 | VIII–IX | Carmona (Sevilla) |
| 09/22/1522 | 02°40′W 36°58′N | >50 | VIII–IX | Alhama de Almería (Almería) |
| 06/19/1644 | 00°25′W 38°48′N | 20–50 | VIII | Muro de Alcoy (Alicante) |
| 10/09/1680 | 04°36′W 36°48′N | 10–20 | VIII–IX | NW Málaga |
| 03/23/1748 | 00°38′W 39°02′N | 10–20 | IX | Estubeny (Valencia) |
| 08/25/1804 | 02°50′W 36°46′N | 10–20 | VIII–IX | Dalías (Almería) |
| 03/21/1829 | 00°41′W 38°05′N | 10–20 | IX–X | Torrevieja (Alicante) |
| 12/25/1884 | 03°59′W 37°00′N | <10 | IX–X | Arenas del Rey (Granada) |

An estimation of the error in the epicentral location is included.

Zones, External Zones, Campo de Gibraltar units, and the Guadalquivir foreland basin. This last unit limits the cordillera from the Iberian Massif to the north (Fig. 2). The External Zones represent the former continental margin of the southern Iberian plate (García Hernández et al., 1980). They have been subdivided into the Subbetic Zone to the south, characterized by pelagic facies, and a Prebetic Zone to the north and east of the previous one, where shallow marine facies are common. The Internal Zones consist of four tectonically superimposed complexes. From bottom to top, they are the Nevado-Filábride, the Alpujárride, the Maláguide, and the Dorsal Complex. The Nevado-Filábride and the Alpujárride show a well-developed Alpine metamorphism. The materials of the Campo de Gibraltar came from the former Flysch basin, originally located to the south of the Internal Zone (Sanz de Galdeano, 1997). In addition to the previous domains, several neogene basins (Granada, Guadix-Baza, Huercal-Overa, Lorca, Cartagena, Low Segura Basin, etc.) exist. They are filled by Upper Miocene to Quaternary sediments. Their creation and evolution are controlled by the tectonic activity in the cordillera.

The tectonic activity and associated seismicity in southern Spain are related to the western boundary between the Eurasian and African plates. According to the NUVEL-1 model (De Mets et al., 1994), the relative motion of compression between Africa and South Spain varies between 4 and 6 mm/year, with a NW–SE to NNW–SSE horizontal direction of compression, combined with a perpendicular NE–SW extension (Sanz de Galdeano, 1990; Galindo Zaldívar et al., 1999; Henares et al., 2003).

In the central sector of the Betic cordillera, characterized by a diffuse, low to moderate seismicity, the most noticeable aspect during the Quaternary is a vertical movement, implying some uplift and radial extension of the cordillera (Sanz de Galdeano and López Garrido, 1991). The Sierra Nevada range is

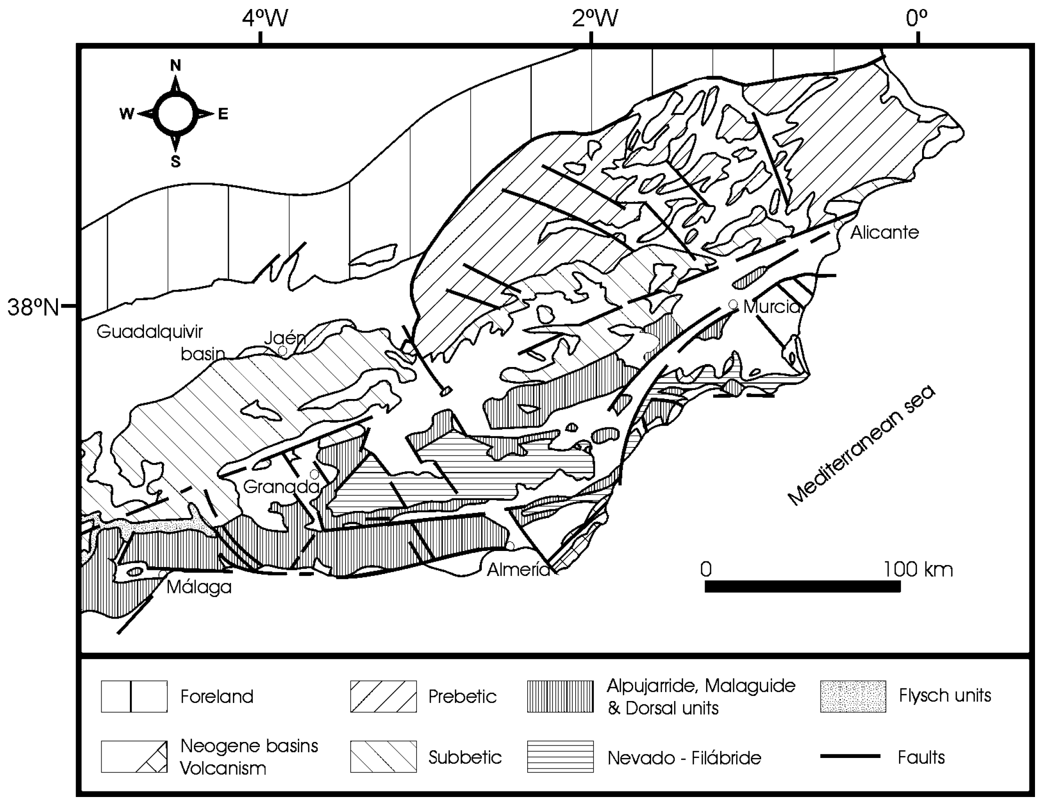


Fig. 2. Tectonic sketch of the region (adapted from Sanz de Galdeano et al., 1995).

suffering extensional uplift along its western and southwestern flanks, with estimated rates of uplift of 0.3 to 0.8 m/ka (Sanz de Galdeano and López Garrido, 1999; García et al., 2003). The extension is produced by normal faults of several orientations, but mainly with a NW–SE strike (Alfaro et al., 2001a; Sanz de Galdeano et al., 2003). Most of them are clearly active, considering that they show evident and very recent geological features of current activity (geomorphologic scarps). There are low-angle faults on the border of Sierra Nevada and more to the south as well. Nevertheless, their importance in generating earthquakes seems to be negligible (Sanz de Galdeano et al., 2003).

In the eastern sector of the cordillera, there is a notable development of strike-slip faults (Sanz de Galdeano, 1983). The main structure in this sector of the cordillera is the so-called Trans-Alborán Shear Zone (Larouzière et al., 1988), also known as Eastern Betic Shear Zone (Silva et al., 1993). It consists of a left-lateral shear zone of sigmoidal geometry which extends from Almería to Alicante (Fig. 2). This area has been struck by some of most destructive earthquakes recorded in Spain (Fig. 3), especially at its terminal splays, the Almería and Alicante sectors. Data coming from geophysics, geomorphology, trenches, and paleoliquefaction studies (Martínez Díaz and Hernández Enrile, 2001; Martínez Díaz et al., 2001) reveal a recent (last 100 ka) uplift of the sector. According to data compiled by Silva et al. (2003), uplift of mountain fronts ranges from 0.03 to 0.15 m/ka in the Almería sector, from 0.04 to 0.08 m/ka in the central sector, and a range of 0.05 m/ka in the Alicante sector. The difficulty in discriminating between seismic and aseismic activity in these data is a problem. Conversely, the data obtained by Alfaro et al. (2001b) from the datation of paleoliquefaction features in Holocene sediments of the Segura river flood plain are of great interest for characterizing the seismic activity of active faults in the Alicante sector. According to their data, an average return period of approximately 1000 years is obtained for earthquakes of moderate to high magnitude ($M_S > 5.0$, without discriminating the maximum possible magnitude for the events nor for the causative fault). Similar return periods are observed when geotechnical data (soil strength) are combined with a probabilistic seismic hazard analysis in the zone (Delgado et al., 1998).

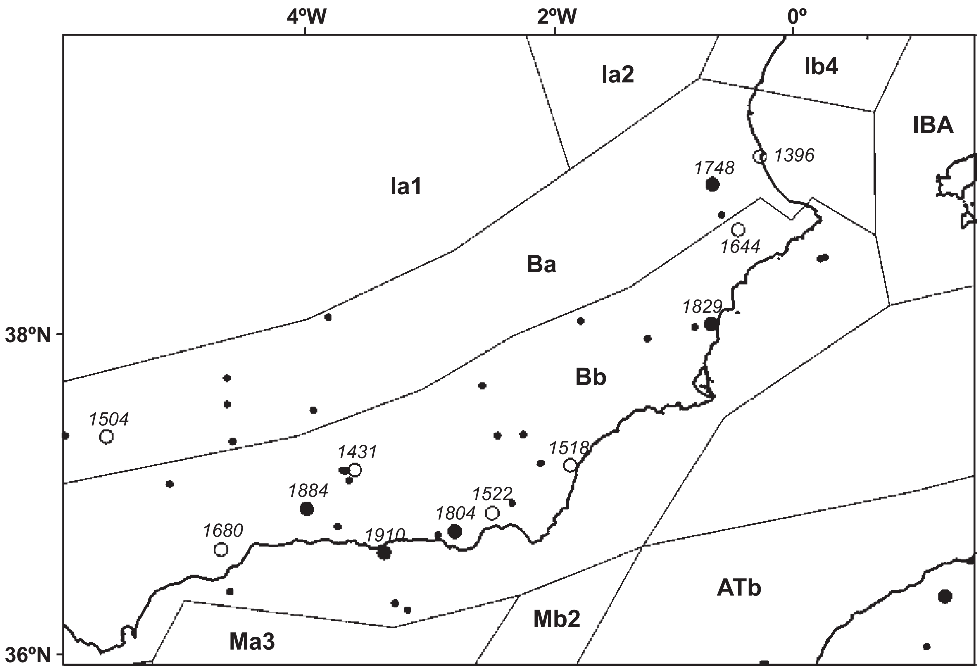


Fig. 3. Seismicity map, including seismogenic sources taken from Peláez and López Casado (2002), showing $4.5 \leq M_S < 5.5$ (small filled circles) and $M_S \geq 5.5$ (large filled circles) earthquakes since 1700 and $M_S \geq 5.5$ earthquakes since 1300 (large open circles).

The geological domains and subdomains proposed as seismic sources in the whole Iberian Peninsula by Peláez and López Casado (2002) have also been used here. The seismogenic sources which most contribute to seismic hazard are those appearing in Fig. 3, especially the called *Ba* (mostly Betic External Zones) and *Bb* (mostly Betic Internal Zones and Northern Alboran Sea) sources. They constitute the Betic Cordilleras. Their main characteristics from the seismic point of view are quoted below.

## 3. Data and methodology

The data and methodology are the same as in a previous assessment of seismic hazard and deaggregation in Spain (Peláez and López Casado, 2002; Peláez et al., 2002), with the exception of the attenuation relationship. The main reason for using spatially smoothed historic seismicity to assess the seismic hazard is the fact that we work with background (also called distributed) seismicity. This method is well adapted to model the seismicity that cannot be assigned to specific geological structures.

Of all the attenuation relations for the Arias intensity reported (e.g., Faccioli, 1983; Wilson and Keefer, 1985; Sabetta and Pugliese, 1987; Wilson, 1993; Kayen and Mitchel, 1997a; Zonno and Montaldo, 2002; Travasarou et al., 2003; Hwang et al., 2004), we consider that the Sabetta and Pugliese (1996) relationship is the most reliable one for our region. The reasons are: (a) the large amount of data used by them; (b) the fact that it allows us to include soil condition information; (c) they use the same magnitude scale, $M_S$, as previous seismic hazard assessments in this region; and (d) the tectonic similarities between our region and the Friuly region, where they collect much of their data. Concerning this last point, the Italian tectonic activity is a result of a somewhat similar geological context as our area of study, i.e., the zone of contact between the Eurasian and African plates. The Friuly region, in the Alpine arc, is characterized by a predominant compressive regime (Romeo and Pugliese, 2000), just like the Betic Cordilleras.

Additionally, it must be reminded that we cannot include in this preliminary assessment the source directivity, as Faccioli (1983) did, nor the fault type, as Travasarou et al. (2003) have done. The reason is that, currently, we have no paleoseismic information to include in the probabilistic assessment. In the region under study, it was impossible to associate the main historic earthquakes (Fig. 3) with active faults. This is the reason why seismicity has been used alone in the assessment, and not seismotectonic (fault) sources. The use of active fault data in the seismic hazard computation at the Granada Basin, in southern Spain, was done in a previous work (Peláez et al., 2003). The fact that part of the movements of the faults were due to a clear aseismic creep, unknown in magnitude over the total slip rate, led to a clear overestimation of the hazard values. Alternatively, relationships including source directivity or fault types are clearly suitable for ground-shaking scenarios using deterministic models.

The Sabetta and Pugliese (1996) relationship has been developed using the horizontal component of the accelerogram with the largest value of Arias intensity. Additionally, the following different geological conditions are considered: (a) stiff rocks, with shear-wave velocity greater than 800 m/s; (b) deep soils ($h>20$ m); and (c) shallow soils ($h\leq 20$ m), both with shear-wave velocity between 400 and 800 m/s. The relationship is represented by the expression

$$\log I_a = a + bM + c\log(R^2 + h^2)^{1/2} + e_1 S_1 + e_2 S_2 \tag{3}$$

where $M$ is the surface wave magnitude, $R$ is the epicentral distance (in km) or fault distance, and $S_1$ and $S_2$ are variables, referring to the geological site classification. $a$, $b$, and $c$ are coefficients, and $h$ is a depth parameter to improve the regression. The variables $e_1$ and $e_2$ are site parameters.

The performance of this attenuation relationship is depicted in Fig. 4, where predicted values of the Arias intensity have been plotted versus distance for different magnitudes and soil conditions, showing their uncertainty (confidence intervals). Moreover, in Fig. 5, a simulation of the predicted values for the most important earthquakes that have taken place in the Granada Basin (Betic Cordilleras, southern Spain) is shown. These are: the 24 April 1431 Atarfe earthquake (5.5 $M_S$) and the 25 December 1884 Arenas del Rey earthquake (5.8 $M_S$; Table 1). The assigned magnitude to the 1431 Atarfe earthquake is the

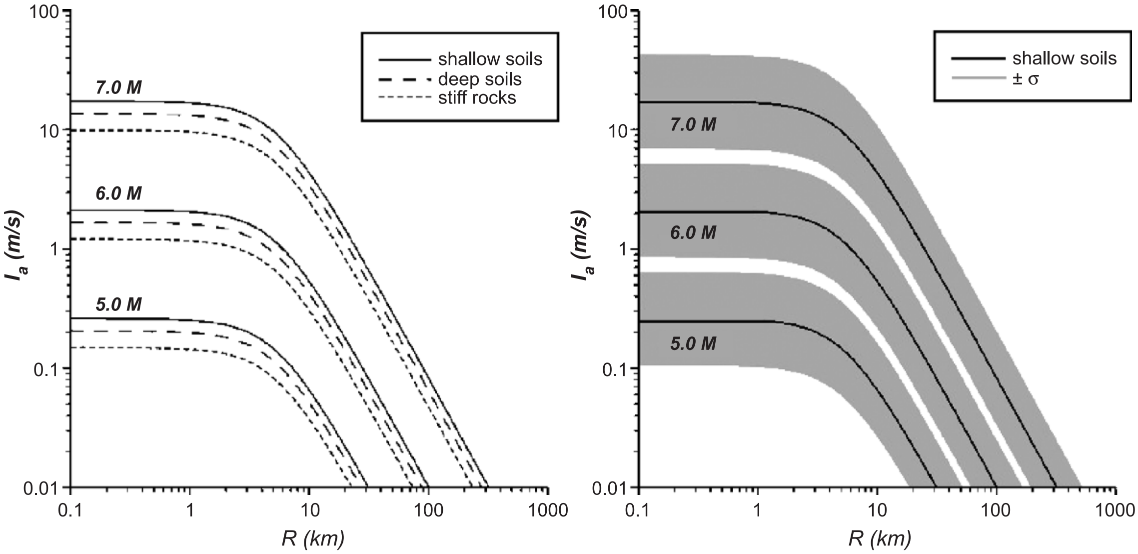


Fig. 4. Predicted values using the Sabetta and Pugliese (1996) relationships. Left: Arias intensity vs. distance for shallow and deep soils and stiff rocks, and for different magnitudes. Right: Arias intensity vs. distance for shallow soils, and for different magnitudes, showing the mean and mean+$\sigma$ curves.

macroseismic magnitude obtained using the relationship between magnitude and intensity by López Casado et al. (2000), specifically developped for the Ibero-Magrebhian region. The assigned magnitude to the 1884 Arenas del Rey earthquake is the one obtained by Molina (1998) using the Ambraseys (1985) procedure, considering the mean radii of the isoseismals.

For the seismic hazard assessment, the Iberian seismic catalog (Mezcua and Martínez Solares, 1983; updated up to 1999) has been used. Peláez and López Casado (2002) discuss the processing of the catalog to be used in the seismic hazard assessment for Spain. The original approach proposed by Frankel (1995) has been modified taking into account the seismic characteristics of the region. A characteristic earthquake model has not been included, because no paleoseismic information exists, nor a background zone. In relation to the method itself, $b$ and $m_{\max}$ values have been smoothed, as proposed by Bender (1986), and the weights by which each considered seismic model contributes to the hazard depend on the return period.

Four Poissonian seismic models, including shallow seismicity ($h<30$ km), have been considered. They include (a) earthquakes with magnitude above $M_S$ 5.5 after 1300, (b) those with magnitude above $M_S$ 4.5 after 1700, (c) those with magnitude above $M_S$ 3.5 after 1920, and (d) those with magnitude above 2.5 after 1960.

Only the seismicity included in the first two models, the largest earthquakes in the last 700 years, appears depicted in Fig. 3. In addition, in this plot, we can see the boundaries of the seismic sources considered in the region (Molina, 1998; Peláez and López Casado, 2002). As stated above, the whole Betic domain, where the main historic earthquakes are included, is divided into the subdomains (seismic sources) *Ba* and *Bb* (Fig. 3), separated by the Cádiz–Alicante fault. The parameter values of the truncated Gutenberg–Richter recurrence relationship for these two seismic sources are the following. $b$ values of 0.55 ($\sigma=0.05$) and 0.67 ($\sigma=0.03$), and $m_{\max}$ values of 6.2 ($\sigma=0.72$) and 7.3 ($\sigma=0.76$) are obtained, respectively, for seismic sources *Ba* and *Bb* (Peláez and López Casado, 2002), using the Weichert (1980) and Pisarenko et al. (1996) procedures. The values quoted above have been obtained using the $M_S$ magnitude.

The seismicity included in each of these four seismic models is counted in a grid with cell dimension of 10 km, and smoothed using a Gaussian

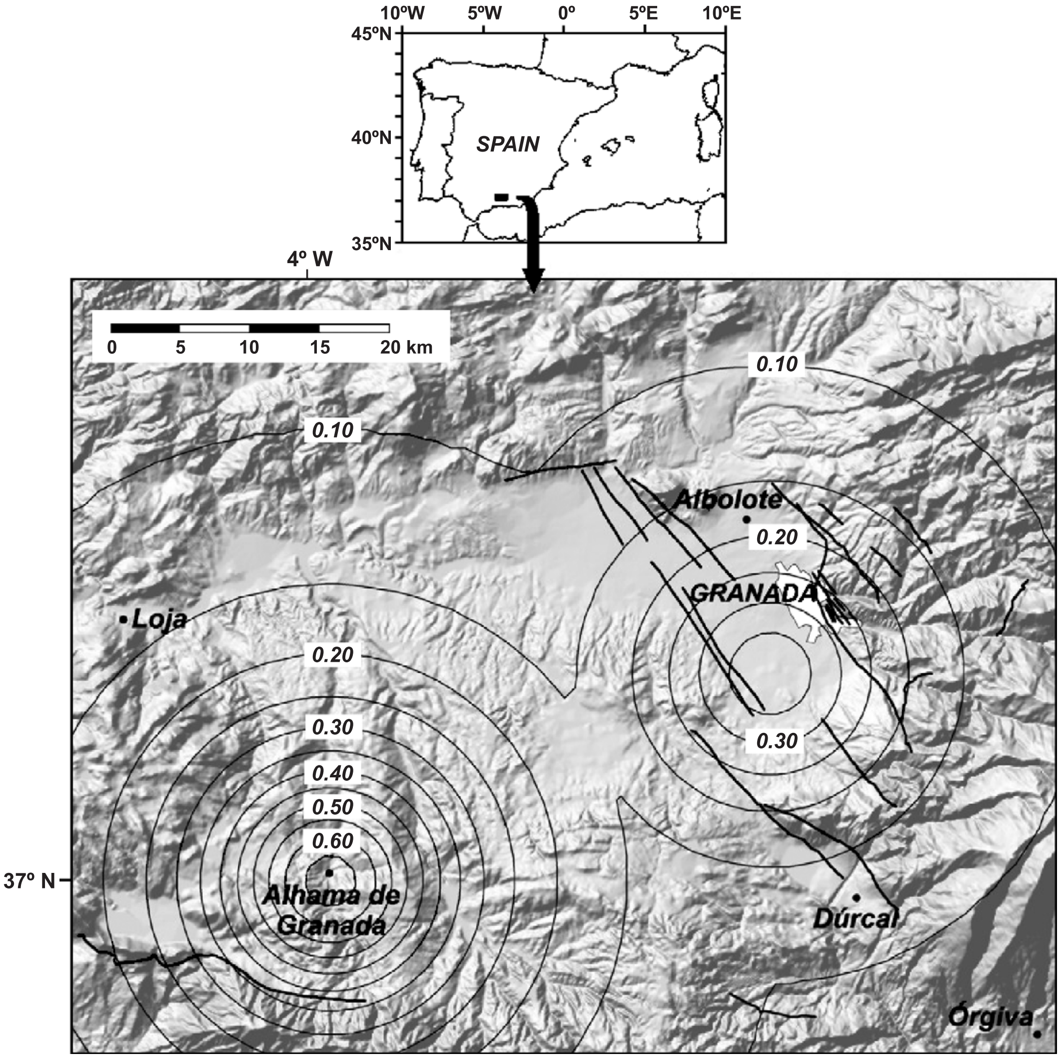


Fig. 5. Arias intensity predicted values, using the Sabetta and Pugliese (1996) relationship for shallow soils, for the 25 December 1884 Arenas del Rey earthquake (to the left) and for the 24 April 1431 Atarfe earthquake (to the right). Active faults in the Granada Basin are shown (taken from Sanz de Galdeano et al., 2003).

function. This function depends on a spatial parameter $c$, called correlation distance, which provides more or less smoothing; $c$ values of 15, 15, 10, and 5 km, respectively, were used. Each earthquake is smoothed into a circle with radius equal to $3c$. Therefore, we consider both the uncertainty in the earthquake location, a key issue when historical earthquakes are included in the assessment, and the fact that an earthquake is not a point process. For example, an $M_S$ 6.0 earthquake included in the first model, in an epoch where macroseismic effects are used to locate its epicenter, is spread into a circle with radius equal to 45 km.

Seismic hazard generated by these four models is calculated using the well-known total probability theorem, expressed in terms of rate of exceedance of a certain level of Arias intensity. The mean Arias intensity values are then derived by weighting the obtained seismic hazards results. The subjective weights used for a 475 years return period, considering the above-mentioned guideline, are 0.3, 0.3, 0.2, and 0.2, respectively.

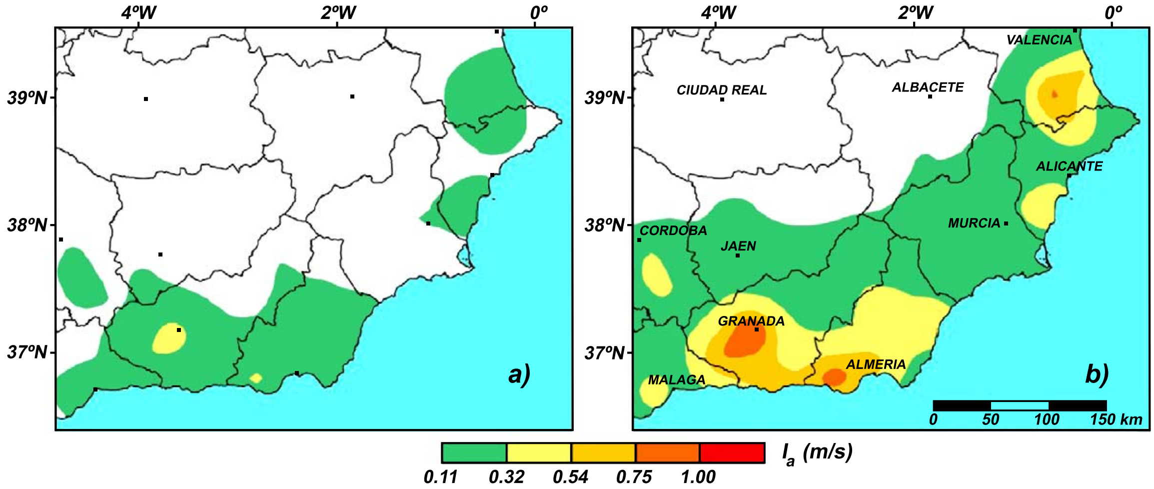


Fig. 6. Seismic hazard maps in terms of Arias intensity in southeastern Spain. Results for shallow soils: (a) using the mean attenuation curve and (b) using the mean + $\sigma$ attenuation curve.

The computation procedure is described in detail in Peláez and López Casado (2002).

## 4. Results

Figs. 6–8 depict the results obtained for the seismic hazard assessment in terms of Arias intensity maps. The computed and depicted Arias intensity is as defined by the Eq. (3). Specifically, we show the probabilistic seismic hazard results for a return period of 475 years. The seismic hazard has been computed using the mean and the mean + $\sigma$ attenuation curves. Therefore, we stress the uncertainty in the result due to the variation in defining the attenuation relationship. The maps corresponding to the mean + $\sigma$ attenuation curve could also be considered as a conservative result for some uses. In addition, specific Arias intensity values for several key areas are reported in Table 2.

The Arias intensity maps in Figs. 6–8 display the contour levels values of 0.11, 0.32, and 0.54 m/s.

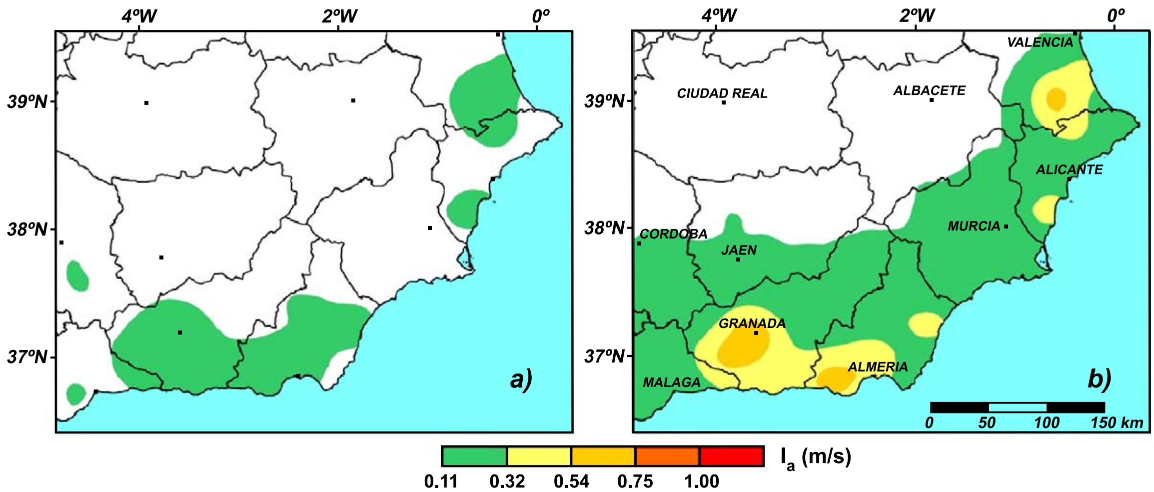


Fig. 7. Seismic hazard maps in terms of Arias intensity in southeastern Spain. Results for deep soils: (a) using the mean attenuation curve and (b) using the mean + $\sigma$ attenuation curve.

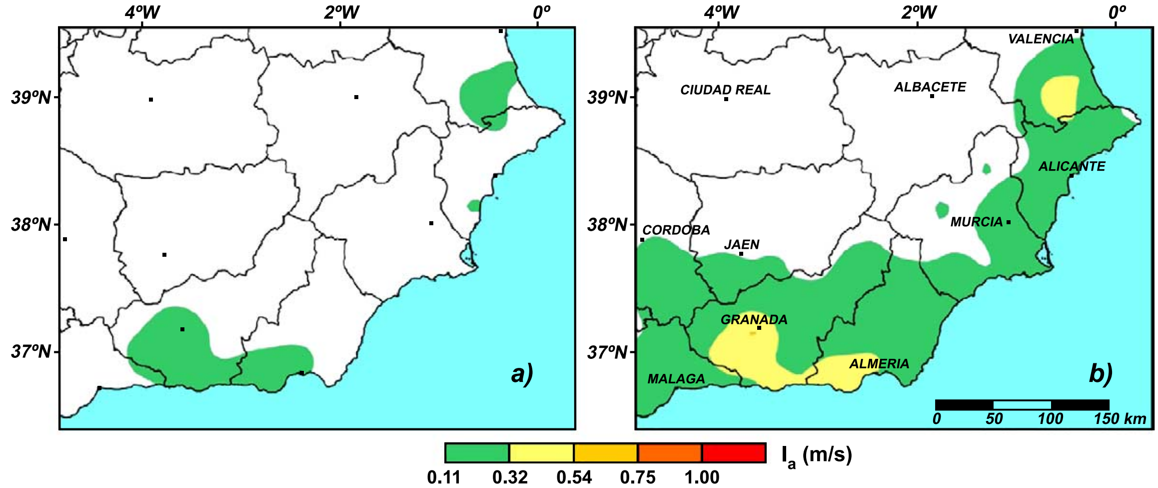


Fig. 8. Seismic hazard maps in terms of Arias intensity in southeastern Spain. Results for stiff rocks: (a) using the mean attenuation curve and (b) using the mean + $\sigma$ attenuation curve.

These values are accepted (Keefer and Wilson, 1989; Harp and Wilson, 1995) as those triggering three different classes of landslides: (a) falls, disrupted slides and avalanches (the most usual ones), (b) slumps, block slides, and earth flows, and (c) lateral spreads and flows. Therefore, by inspection of the maps, we can know the worst likely landslide type that may occur.

Figs. 6–8 identify the regions with higher seismic hazard. As expected, we find a strong correlation between these figures and Fig. 1, where the seismic hazard in terms of mean PGA is shown. Areas having mean PGA values above 1.2 and 2.0 m/s$^2$ correlate well with areas having Arias intensity values above 0.11 and 0.32 m/s, respectively, for shallow soil sites. Mean PGA values above 1.4 m/s$^2$ correlate with Arias intensity values above 0.11 m/s, for deep soil sites, and mean PGA values above 1.6 m/s$^2$ correlate with Arias intensity values above 0.11 m/s, for hard rocks. The shape of the seismic hazard maps, both in terms of Arias intensity and mean PGA, remains constant. Evidently, not the values.

The four areas with greatest seismic hazard are shown in Table 2. The Granada Basin, to the SW of Granada, shows the greatest seismic hazard values, of the order of those obtained in most of the Italian Apennine chain (Romeo, 2000; Romeo and Pugliese, 2000). This area has suffered the 1431 Atarfe earthquake ($I$ = VIII–IX) and the 1884 Arenas del Rey earthquake (IX–X), among others (see Fig. 3 and Table 1). The next important area is the SW of Almería. In this area, the 1522 Alhama de Almería earthquake and the 1804 Dalías earthquake, both with maximum assigned intensity of VIII–IX, occurred. The next one is the south of Valencia area, with seismic hazard values similar to the SW of Almería

Table 2
Obtained Arias intensity maximum values in four selected areas for a return period of 475 years

| Area | PGA (m/s$^2$) | $I_a$ (m/s) | | | | | |
|---|---|---|---|---|---|---|---|
| | | Shallow soils | | Deep soils | | Stiff rocks | |
| | | Mean | Mean + $\sigma$ | Mean | Mean + $\sigma$ | Mean | Mean + $\sigma$ |
| Granada Basin | 2.25 | 0.38 | 0.95 | 0.30 | 0.75 | 0.22 | 0.54 |
| SW Almería | 2.09 | 0.33 | 0.83 | 0.26 | 0.65 | 0.19 | 0.47 |
| S Valencia | 2.09 | 0.30 | 0.76 | 0.24 | 0.60 | 0.18 | 0.43 |
| S Alicante | 1.81 | 0.20 | 0.50 | 0.16 | 0.40 | 0.12 | 0.29 |

The results using the mean and the mean + $\sigma$ attenuation curves are listed. We also show, as a comparison and reference, the seismic hazard in terms of mean PGA (Peláez and López Casado, 2002).

zone. This area has experienced the 1396 Tabernes de Valldigna earthquake (VIII–IX), the 1644 Muro de Alcoy earthquake (VIII), and the 1748 Estubeny earthquake (IX). Finally, the south of Alicante shows lower seismic hazard that in the previous sites. The 1829 Torrevieja earthquake (IX–X) took place in this area. The above-cited macroseismic intensity values (Table 1) are in the EMS-98 macroseismic scale (Grüntal, 1998) and are those that appear in a recent revision and comprehensive study of the pre-1900 period of the Iberian earthquake catalog (Martínez Solares and Mezcua, 2002).

## 5. Summary and final discussion

For the first time, probabilistic seismic hazard values in terms of Arias intensity for southeastern Spain have been computed. The spatially smoothed seismicity procedure has been used (Peláez and López Casado, 2002). Maps, for different soil conditions, are presented for a return period of 475 years. The main aim of this work is to show which are the seismically triggered landslide prone areas in this region, using a probabilistic model.

The total uncertainty has not been considered in this work. Only the effect of the attenuation uncertainty is included. As in any seismic hazard assessment, several factors, some more significant than others, contribute to the final uncertainty. Among them, we have the delimitation in seismic sources, the spanning and quality of the catalog, or the computed parameters needed in some stages of the computation. In any case, we are fully confident that the proposed approach, considering earthquakes where they have taken place, decreases the model uncertainty, as has been emphasized by several authors. New improvements of the historic Spanish catalog, adding the paleoseismic events, and an attenuation relationship for the Arias intensity specifically developed for the region, will allow us a more reliable evaluation of the seismic hazard values.

Typical values for a moderate seismic hazard region have been obtained, that is, above 0.1 m/s in most of Betic Cordilleras, considering shallow soils. The greatest seismic hazard value reached is of the order of 0.4 m/s in the Granada Basin, the most seismically active region in Spain. This is due to several significant historic earthquakes located in this area. In any case, taking into account the uncertainty in the attenuation relationships, higher probabilistic values could be attained.

Future studies including also the geology, geotechnical properties, and the slope gradient, i.e., soil conditions and site effects, will further a landslide prediction model (Murphy et al., 2002; Havenith et al., 2003).

## Acknowledgments

The authors wish to thank the very helpful review provided by W. Murphy. This research was partially supported by the Seismic Hazard and Microzonification Research Group of the Junta de Andalucía in Spain RNM-0217 and the project RIES-CTIDIB/2002/177.

## References

Abdrakhmatov, K., Havenith, H.B., Delvaux, D., Jongmans, D., Trefois, P., 2003. Probabilistic PGA and Arias intensity maps of Kyrgyzstan (Central Asia). J. Seismol. 7, 203–220.

Alfaro, P., Galindo Zaldívar, J., Jabaloy, A., López Garrido, A.C., Sanz de Galdeano, C., 2001. Evidence for the activity and paleoseismicity of the Padul fault (Betic Cordillera, southern Spain). Acta Geol. Hisp. 36, 283–295.

Alfaro, P., Delgado, J., Estévez, A., López Casado, C., 2001. Paleoliquefaction in the Bajo Segura basin (eastern Betic Cordillera). Acta Geol. Hisp. 36, 233–244.

Ambraseys, N.N., 1985. Intensity-attenuation and magnitude-intensity relationships for Northwest European earthquakes. Earthq. Eng. Struct. Dyn. 13, 733–778.

Arias, A., 1970. A measure of earthquake intensity. In: Hansen, R.J. (Ed.), Seismic Design for Nuclear Power Plants. MIT Press, Cambridge, MA, pp. 438–483.

Bender, B., 1986. Modeling source zone boundary uncertainty in seismic hazard analysis. Bull. Seismol. Soc. Am. 76, 329–341.

Cabañas, L., Benito, B., Herráiz, M., 1997. An approach to the measurement of the potential structural damage of earthquake ground motion. Earthq. Eng. Struct. Dyn. 26, 79–92.

Carro, M., De Amicis, M., Luzi, L., Marzorati, S., 2003. The application of predictive modeling techniques to landslides induced by earthquakes: the case study of the 26 September 1997 Umbria–Marche earthquake (Italy). Eng. Geol. 69, 139–159.

Corominas, J., 1993. Spatial prediction of landslides. In: Nemec, J., Nigg, J.M., Siccardi, F. (Eds.), Prediction and Perception of Natural Hazards. Kluwer Academic Publishers, Dordrecht, pp. 125–132.

De Mets, C., Gordon, R.G., Argus, D.F., Stein, S., 1994. Effect of recent revisions to the geomagnetic reversals time scale on estimates of current plate motions. Geophys. Res. Lett. 21, 2191–2194.

Del Gaudio, V., Pierri, P., Wasowski, J., 2003. An approach to time-probabilistic evaluation of seismically induced landslide hazard. Bull. Seismol. Soc. Am. 93, 557–569.

Delgado, J., López Casado, C., Alfaro, P., Giner, J., Estévez, A., 1998. Liquefaction potential in the Lower Segura basin (Southeast Spain). Eng. Geol. 49, 61–79.

Faccioli, E., 1983. Measures of strong ground motion derived from a stochastic source model. Soil Dyn. Earthqu. Eng. 2, 135–149.

Faccioli, E., 1995. Induced hazards: earthquake triggered landslides. In: Proceedings of the Fifth International Conference on Seismic Zonation, Nice, France, 17–19 October 1995 vol. III. pp. 1908–1931.

Frankel, A., 1995. Mapping seismic hazard in the Central and Eastern United States. Seismol. Res. Lett. 66, 8–21.

Galindo Zaldívar, J., Jabaloy, A., Serrano, I., Morales, J., González Lodeiro, F., Torcal, F., 1999. Recent and present-day stresses in the Granada basin (Betic Cordilleras): example of a late Miocene–present-day extensional basin in a convergent plate boundary. Tectonics 18, 686–702.

García, A.F., Zhu, Z., Ku, T.L., Sanz de Galdeano, C., Chadwick, O.A., Chacón Montero, J., 2003. Tectonically driven landscape development within the eastern Alpujarran Corridor, Betic Cordillera, SE Spain (Almería). Geomorphology 50, 83–110.

García Hernández, M., López Garrido, A.C., Rivas, P., Sanz de Galdeano, C., Vera, J.A., 1980. Mesozoic paleogeographic evolution of the External Zones of the Betic Cordillera. Geol. Mijnb. 59, 155–168.

Grüntal, G. (Ed.), 1998. European macroseismic scale 1998, vol. 15. Centre Européen de Géodynamique et de Séismologie, Cahiers du Centre Européen de Géodynamique et de Séismologie, Luxembourg.

Harp, E.L., Wilson, R.C., 1995. Shaking intensity thresholds for rock falls and slides: evidence from 1987 Whittier Narrows and Superstition Hills earthquake strong-motion records. Bull. Seismol. Soc. Am. 85, 1739–1757.

Havenith, H.B., Vanini, M., Jongmans, D., Faccioli, E., 2003. Initiation of earthquake-induced slope failure: influence of topographical and other site specific amplification effects. J. Seismol. 7, 397–412.

Henares, J., López Casado, C., Sanz de Galdeano, C., Delgado, J., Peláez, J.A., 2003. Stress fields in the Iberian–Maghrebi region. J. Seismol. 7, 65–78.

Hwang, H., Lin, C.K., Yeh, Y.T., Cheng, S.N., Chen, K.C., 2004. Attenuation relations of Arias intensity based on the Chi-Chi Taiwan earthquake data. Soil Dyn. Earthqu. Eng. 24, 509–517.

Jibson, R.W., Harp, E.L., Michael, J.A., 1998. A method for producing digital probabilistic seismic landslides hazard maps: an example from the Los Angeles, California, area. US Geological Survey Open-File Report. U.S. Government Printing Office, Washington, DC, pp. 98–113.

Jibson, R.W., Harp, E.L., Michael, J.A., 2000. A method for producing digital probabilistic seismic landslides hazard maps. Eng. Geol. 58, 271–289.

Kayen, R.E., Mitchel, J.K., 1997. Assessment of liquefaction potential during earthquakes by Arias intensity. J. Geotech. Geoenviron. Eng. 123, 1162–1174.

Kayen, R.E., Mitchel, J.K., 1997. Arias intensity assessment of liquefaction test sites on the east side of San Francisco Bay affected by the Loma Prieta, California, earthquake of 17 October 1989. Nat. Hazards 16, 243–265.

Keefer, D.K., 2002. Investigating landslides caused by earthquakes. A historical review. Surv. Geophys. 23, 473–510.

Keefer, D.K., Wilson, R.C., 1989. Predicting earthquake-induced landslides, with emphasis on arid and semi-arid environments. In: Sadler, P.M., Morton, D.M. (Eds.), Landslides in a Semi-Arid Environment, vol. 2. Inland Geological Society, pp. 118–149.

Larouzière, D., Bolze, J., Bordet, P., Hernández, J., Montenat, C., Ott d'Estovou, P., 1988. The betic segment of the lithospheric Transalboran Shear zone during the Late Miocene. Tectonophysics 152, 41–52.

López Casado, C., Molina, S., Giner, J.J., Delgado, J., 2000. Magnitude-Intensity relationships in the Ibero-Magrebhian region. Nat. Hazards 22, 269–294.

Margottini, C., Molin, D., Serva, L., 1992. Intensity versus ground motion: a new approach using Italian data. Eng. Geol. 33, 45–58.

Martínez Díaz, J.J., Hernández Enrile, J.L., 2001. Using travertine deformations to characterize paleoseismic activity along an active oblique-slip fault: the Alhama de Murcia fault (Betic Cordillera, Spain). Acta Geol. Hisp. 36, 297–314.

Martínez Díaz, J.J., Masana, E., Hernández Enrile, J.L., Santanach, P., 2001. Evidence for coseismic events of recurrent prehistoric deformation along the Alhama de Murcia fault, southeastern Spain. Acta Geol. Hisp. 36, 315–328.

Martínez Solares, J.M., Mezcua, J., 2002. Seismic catalog of the Iberian peninsula (880 BC-1900) (in Spanish). Report. Instituto Geográfico Nacional, Madrid.

Mezcua, J., Martínez Solares, J.M., 1983. Seismicity of the Ibero-Maghrebian area (in Spanish). Report. Instituto Geográfico Nacional, Madrid.

Molina, S., 1998. Seismotectonic and seismic hazard in the limit between Iberia and Africa (*in Spanish*). PhD thesis. University of Granada, Spain.

Murphy, W., Petley, D.N., Bommer, J., Mankelow, J.M., 2002. Uncertainty in ground motion estimates for the evaluation of slope stability during earthquakes. Q. J. Eng. Geol. Hydrogeol. 35, 71–78.

Newmark, N.M., 1965. Effects of earthquakes on dams and embankments. Geotechnique 15, 139–160.

Peláez, J.A., López Casado, C., 2002. Seismic hazard estimate at the Iberian Peninsula. Pure Appl. Geophys. 159, 2699–2713.

Peláez, J.A., López Casado, C., 2004. Seismic hazard and deaggregration at the nuclear power plant sites in Spain. Nat. Hazards (submitted for publication).

Peláez, J.A., López Casado, C., Henares, J., 2002. Deaggregation in magnitude, distance and azimuth in the south and west of the Iberian Peninsula. Bull. Seismol. Soc. Am. 92, 2177–2185.

Peláez, J.A., Sanz de Galdeano, C., López Casado, C., 2003. Use of active fault data versus seismicity data in the evaluation of seismic hazard in the Granada Basin (Southern Spain). Bull. Seismol. Soc. Am. 93, 1670–1678.

Pisarenko, V.F., Lyubushin, A.A., Lysenko, V.B., Golubeva, T.V., 1996. Statistical estimation of seismic hazard parameters: maximum possible magnitude and related parameters. Bull. Seismol. Soc. Am. 86, 691–700.

Romeo, R., 2000. Seismically induced landslide displacements: a predictive model. Eng. Geol. 58, 337–351.

Romeo, R., Pugliese, A., 2000. Seismicity, seismotectonics and seismic hazard of Italy. Eng. Geol. 55, 241–266.

Sabetta, F., Pugliese, A., 1987. Attenuation of peak horizontal acceleration and velocity from Italian strong-motion records. Bull. Seismol. Soc. Am. 77, 1491–1513.

Sabetta, F., Pugliese, A., 1996. Estimation of response spectra and simulation of nonstationary earthquake ground motions. Bull. Seismol. Soc. Am. 86, 337–352.

Sanz de Galdeano, C., 1983. Los accidentes y fracturas principales de las cordilleras béticas. Estud. Geol. 41, 59–68.

Sanz de Galdeano, C., 1990. Geologic evolution of the Betic Cordilleras in the Western Mediterranean, Miocene to the present. Tectonophysics 172, 107–119.

Sanz de Galdeano, C., 1997. La Zona Interna Bético-Rifeña. Universidad de Granada, Granada, Spain.

Sanz de Galdeano, C., López Garrido, A.C., 1991. Tectonic evolution of the Malaga basin (Betic Cordillera). Regional implications. Geodin. Acta 5, 173–186.

Sanz de Galdeano, C., López Garrido, A.C., 1999. Nature and impact of the Neotectonic deformation in the western Sierra Nevada (Spain). Geomorphology 30, 259–272.

Sanz de Galdeano, C., López Casado, C., Delgado, J., Peinado, M.A., 1995. Shallow seismicity and active faults in the Betic Cordillera: a preliminary approach to seismic sources associated with specific faults. Tectonophysics 248, 293–302.

Sanz de Galdeano, C., Peláez, J.A., López Casado, C., 2003. Seismic potential of the main active faults in the Granada Basin (southern Spain). Pure Appl. Geophys. 160, 1537–1556.

Silva, P.G., Goy, J.L., Somoza, L., Zazo, C., Bardají, T., 1993. Landscape response to strike-slip faulting linked to collisional settings: quaternary tectonics and basin formation in the Eastern Betics, Southeast Spain. Tectonophysics 224, 289–303.

Silva, P.G., Goy, J.L., Zazo, C., Bardají, T., 2003. Fault-generated mountain fronts in southeast Spain: geomorphologic assessment of tectonic and seismic activity. Geomorphology 50, 203–225.

Travasarou, T., Bray, J.D., Abrahamson, N.A., 2003. Empirical attenuation relationship for Arias intensity. Earthq. Eng. Struct. Dyn. 32, 1133–1155.

Weichert, D.H., 1980. Estimation of the earthquake parameters for unequal observation period for different magnitudes. Bull. Seismol. Soc. Am. 70, 1337–1346.

Wilson, R.C., 1993. Relation of Arias intensity to magnitude and distance in California. U.S. Geological Survey Open-File Report. U.S. Government Printing Office, Washington, DC, pp. 93–556.

Wilson, R.C., Keefer, D.K., 1985. Predicting areal limits of earthquake-induced landsliding. In: Ziony, J.I. (Ed.), Evaluating Earthquake Hazards in the Los Angeles Region. An Earth-Science Perspective, U.S. Geological Survey Professional Paper, vol. 1360. U.S. Government Printing Office, Washington, DC, pp. 317–345.

Zonno, G., Montaldo, V., 2002. Analysis of strong ground motions to evaluate regional attenuation relationships. Ann. Geophys. 45, 439–454.